A Novel Low Complexity Local Hybrid Pseudo-SSIM-SATD Distortion Metric Towards Perceptual Rate Control

Yetish G. Joshi*, Jonathan Loo*, Purav Shah*, Shahedur Rahman* and Yoong Choon Chang †
* Computer and Communications Engineering, School of Science and Technology, Middlesex University, London NW4 4BT
{y.joshi, j.loo, p.shah, s.rahman}@mdx.ac.uk
† Faculty of Engineering, Multimedia University, Persiaran Multimedia, 63100 Cyberjaya, Selangor, Malaysia
ycchang@mmu.edu.my

***Abstract*—The front-end block-based video encoder applies an Image Quality Assessment (IQA) as part of the distortion metric. Typically, the distortion metric applies uniform weighting for the absolute differences within a Sub-Macroblock (Sub-MB) at any given time. As video is predominately designed for Humans, the distortion metric should reflect the Human Visual System (HVS). Thus, a perceptual distortion metric (PDM), will lower the convex hull of the Rate-Distortion (R-D) curve towards the origin, by removing perceptual redundancy and retaining perceptual clues. Structured Similarity (SSIM), a perceptual IQA, has been adapted via logarithmic functions to measure distortion, however, it is restricted to the Group of Picture level and hence unable to adapt to the local Sub-MB changes. This paper proposes a Local Hybrid Pseudo-SSIM-SATD (LHPSS) Distortion Metric, operating at the Sub-MB level and satisfying the Triangle Equality Rule (⩤). A detailed discussion of LHPSS's Psuedo-SSIM model will illustrate how SSIM can be perceptually scaled within the distortion metric space of SATD using non-logarithmic functions. Results of HD video encoded across different QPs will be presented showing the competitive bit usage under IbBbBbBbP prediction structure for similar image quality. Finally, the mode decision choices superimposed on the Intra frame will illustrate that LHPSS lowers the R-D curve as homogeneous regions are represented with larger block size.**

I. Introduction

The role of the front-end block-based video encoder is to select the prediction representing the most amount of pixel image block as signalling, for the least amount of distortion for the quantised residue. This is reflected by the Rate-Distortion (R-D) curve in equation (1) within [1]. Here, lambda (λ) applies quantisation to maintain a given bit rate (R), while its effects are assessed by the distortion metric (D). This can extend along various stages of the encoder [2], searching for $J_{min\,energy}$, the optimum point of operation along the convex hull of the R-D curve for the encoder as discussed in [3].

$$J_{min\,energy} = \lambda_{quant} \times R_{bit\,rate} + D_{dist\,metric} \qquad (1)$$

The benefits of having a distortion metric based upon the HVS (perceptual model) can bring the convex hull closer to the origin, thus lowering the bit-rate required to achieve similar Image Quality (IQ) [3], [4]. However, perceptual models can be computationally high and their perceptual distortion scores difficult to quantify [4], hence, the use of low complex tractable solutions [3], which support the Triangle Equality Rule (⩤) [5].

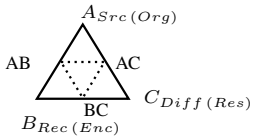

Fig. 1. Triangle Equality

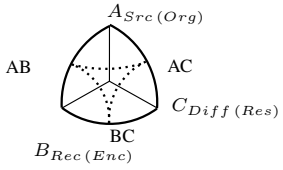

Fig. 2. Geodesic Triangle Equality

The triangle equality rule (⩤) in terms of the distortion metric is where for an image triplet of original, predicted and difference; the distortion score of each pair should be such that the distortion score of one should equate to the summation of the other two distortion scores as shown in figure 1 [5].

Different perceptual based models have achieved the goal of lowering the convex hull towards the origin, such as Just Noticeable Distortion (JND) [6]. JND is highly complex and considers relative lighting conditions, an aspect of HVS. Structural Similarity (SSIM) [7], a low complexity perceptual Image Quality Assessment (IQA) that takes into account the structural information based on relative lighting conditions and is described in equation (2),

$$SSIM(org,rec) = \frac{(2\mu_{org}\mu_{rec}+C_1)\times(2\sigma_{org,rec}+C_2)}{(\mu_{org}^2+\mu_{rec}^2+C_1)\times(\sigma_{org}^2+\sigma_{rec}^2+C_2)} \qquad (2)$$

where, μ_{org} and μ_{rec} represent the mean of the original image block and reconstructed image block, $\sigma_{org}^2$and σ_{rec}^2 are the standard deviations respectively, $\sigma_{org,rec}$ is the covariance, C_1 and C_2 are constants which are calculated based upon the bit depth to stabilise the equation.

It was explained in [5], that a true distortion metric supports the triangle equality rule (⩤), suggesting that SSIM should support a Geodesic Triangle Equality, as shown in figure 2, over a curved space. Hence, non-linear equations should be applied to SSIM to scale it such that it satisfies the triangle equality rule (⩤).

SSIM is a perceptual IQA, but cannot be natively used as a distortion metric as it does not support the triangle equality

rule ($\trianglelefteq$). The efforts of adapting SSIM to operate as a pseudo-distortion metric have been achieved in [8] by use of logarithmic functions, however this approach is limited to the Group of Pictures (GOP) level. Furthermore, it does not meet the goals of low complexity and variability [3]. Variability distinguishes two similar results by their scores, which when considered at the Sub-Macroblock (Sub-MB) level at the Prediction and Mode Decision stages, is crucial. Hence, the accuracy and coverage of a perceptual distortion metric (PDM) must be sufficient to achieve this for the selection of prediction modes and block sizes. The scaled-SSIM-PDM is the evidence backed concept of representing SSIM values within the Standard Traditional Distortion Metrics (STDM) space, proposed in [2]. Though no means of realising this concept was shown, the work highlighted that logarithmic functions should be avoided. Similar to IQA, perceptual vs. non-perceptual, a scaled-SSIM-PDM vs. a non-PDM will differ by the ordering of scores, allowing for certain types of distortions over others [7]. This can be extended at the local level, where the scaling can be adapted according to the perceptual or bit-budget conditions at that given time. Therefore, equation (1) can be re-written as equation (3), where kappa ($\boldsymbol{\kappa}$) represents adapting the scaling of the PDM towards a perceptual rate control (PRC). Rather than adjusting λ to regulate the bit-budget, $\boldsymbol{\kappa}$ can influence the PDM based upon the perceptual significance of the incoming MB [2].

$$J_{min\,energy} = \lambda_{quant} \times R_{bit\,rate} + \boldsymbol{\kappa} \times D_{dist\,metric} \quad (3)$$

Hence, this paper will demostrate SSIM scaled in the distortion metric space of SATD at the Sub-MB level, avoiding logarithmic functions. This will be shown in the form of Pseudo-SSIM and as part of Local Hybrid Pseudo-SSIM-SATD (LHPSS) Distortion Metric which falls back to SATD when Pseudo-SSIM is out of scope.

The paper is divided up as follows, an explanation of how covariance can aid in ordering samples that occupy the same SSIM value, thus allowing SSIM to be scaled and to meet the triangle equality rule ($\trianglelefteq$). However, covariance should be perceptually compared to a HVS model like Just Noticeable Distortion (JND) [6] to assess how it perceptually evaluates an image. Then, a flowchart and operational block diagram will illustrate the Local Hybrid Pseudo-SSIM-SATD (LHPSS) Distortion Metric and Pseudo-SSIM operations in figure 6 and section IV respectively. Finally, the results of the implemented LHPSS, in terms of table of results and Intra frames with mode decision superimposed shown in table I and figure 8 respectively. Please note that the scaling values of Pseudo-SSIM are provided in tables II to XIV.

II. Ordering of SSIM within an existing Distortion Metric Space

It is shown in [5] that SSIM must be non-negative, symmetrical and fulfil the triangle equality rule ($\trianglelefteq$). These first two conditions are met by presenting SSIM in the form of (1-SSIM), a method adopted in [8] and explained in [5]. To support the triangle equality rule ($\trianglelefteq$), the findings in [2] of a universal bounded region (UBR) by block size is extended in this paper by stating how they may be ordered.

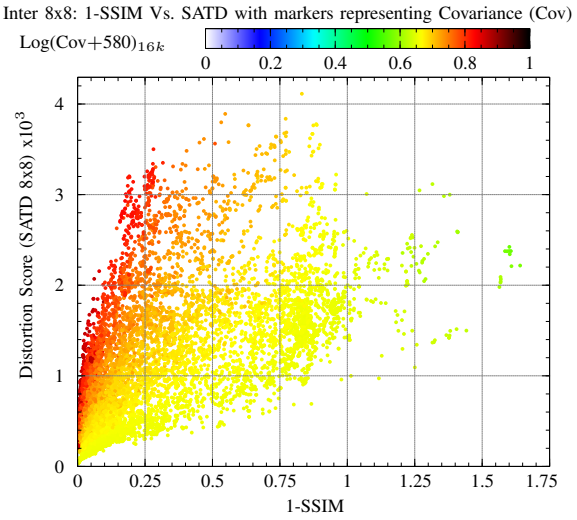

Fig. 3. SSIM vs. SATD (8x8) with Covariance.

The graph in figure 3 illustrates SSIM samples taken along side SATD samples at the Prediction level, with the markers coloured by their covariance (Cov) value. Covariance is a component of SSIM, calculated between the original and reconstructed block as shown in equation (2). In terms of 8-bit Grey-scale, Luma, the theoretical range for Covariance is $\pm$16k. In the graph figure 3, the actual range observed were between -334 and 4731, hence the covariance value has been shifted by $+580$, ($C_2 \times 10$), so that negative covariance values can be illustrated on the same graph. From figure 3, it shows how samples that occupy the same SSIM value can be distinguished by their covariance value. Thus, figure 3 provides insight of how the concept of a scaled-SSIM-PDM in [2] can be achieved within distortion metric of SATD and thus satisfying the triangle equality rule ($\trianglelefteq$).

For reasons of time and simplicity, the modelling of figure 3 in terms of Pseudo-SSIM will be bounded, where $0 \leq \text{Cov} < 8000$ and where $1-\text{SSIM} < 1$. This should cover the majority of samples as shown in [2], however when out of scope of Psuedo-SSIM it will falling back to SATD .

Pseudo-SSIM model will enable prediction and mode decision to assess in terms of the perceptual score at the Sub-MB level. This can be further extended in the form of perceptual rate control as described in equation (3).

III. Covariance Map Analysis

In order to assess the perceptual nature of covariance, a covariance heatmap based upon raw Luma values was produced using a spreadsheet. This was based upon raw Luma values of original and reconstructed intra frames, the covariance range was shifted by three to ensure full coverage. Figure 4 represents the values of covariance in a heat map format with a scale of $Log_{8000}(Cov + 3)$.

The Covariance Map illustrates flat regions with low covariance and where edges or boundaries exist, represented by high covariance. To compare the perceptual covariance

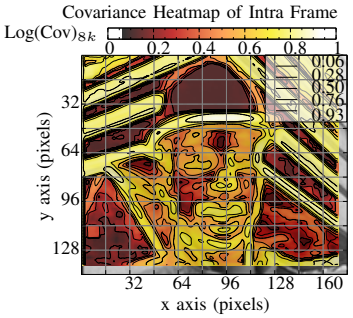

Fig. 4. Covariance Heatmap of Intra Frame (Foreman frame 0 QCIF).

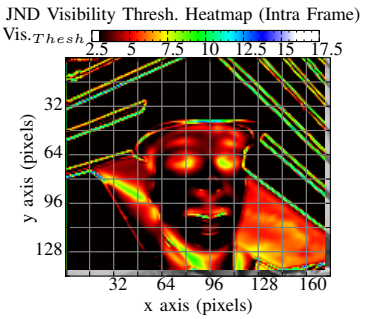

Fig. 5. Just Noticeable Distortion (JND) Visibility Threshold of Intra Frame.

heatmap in HVS terms, another heatmap representing JND using [6] was produced based upon raw luma values and a spreadsheet. The JND heatmap is shown figure 5 illustrates the visibility threshold to be lowest in the homogeneous regions, i.e. the bottom left hand corner, the helmet and upon the panelling. These have the darkest region, where the sensitivity to Luma differences are high and most noticeable. Overall, analysing figure 4 and figure 5 shows that covariance makes a reasonable approximation of JND. This justifies covariance as a perceptual means of scaling of SSIM values. Furthermore, this understanding of interpreting local covariance values of original and reconstructed images can be used to interpret the graphs shown in [2].

IV. Local Hybrid Pseudo-SSIM-SATD (LHPSS) Distortion Metric

Within the encoding process, the Local Hybrid Pseudo SSIM-SATD (LHPSS) model will affect both the intra and inter blocks at the mode and prediction levels and can be extended to Rate Control as part of the PRC model [2].

As Pseudo-SSIM has been defined as where $1-\text{SSIM}<1$ and $0\leq\text{Cov}<8000$, it must work in a Hybrid form along side the distortion metric it mimics, SATD, as a fall-back to ensure full coverage. Figure 6 represents a flowchart of the LHPSS Distortion Metric. Within the flowchart, the Absolute Mean Difference ($|\mu_{O-R}|$) and Covariance are used to provide variableness and scale SSIM respectively. Variableness between samples is crucial for the encoder to distinguish between similar samples [3], especially at the Sub-MB level where the likelihood of prediction modes sharing the same SSIM score is high [2].

The workflow of LHPSS as shown in figure 6 uses SSIM's own components to scale Pseudo-SSIM. The scaling is performed using linear equations to ensure processor friendly operations. Compared to [8], LHPSS can operate locally without using logarithmic functions and without re-quantising to produce a temporal relative distortion scale. As LHPSS operates in the distortion metric space of SATD it satisfies the triangle equality rule ($\trianglelefteq$). Therefore, in [8] the perceptual model must be actively updated on a key frame basis as its relative nature limits the scope to the GOP level or when there is high activity. Hence, in [8] it does not adapt to the local conditions like an STDM. LHPSS distortion metric

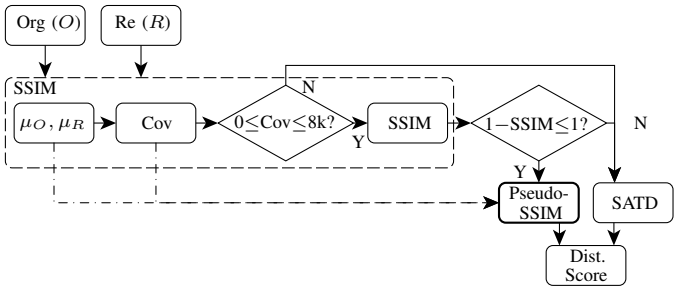

Fig. 6. Flowchart of Hybrid Pseudo-SSIM-SATD Distortion Metric.

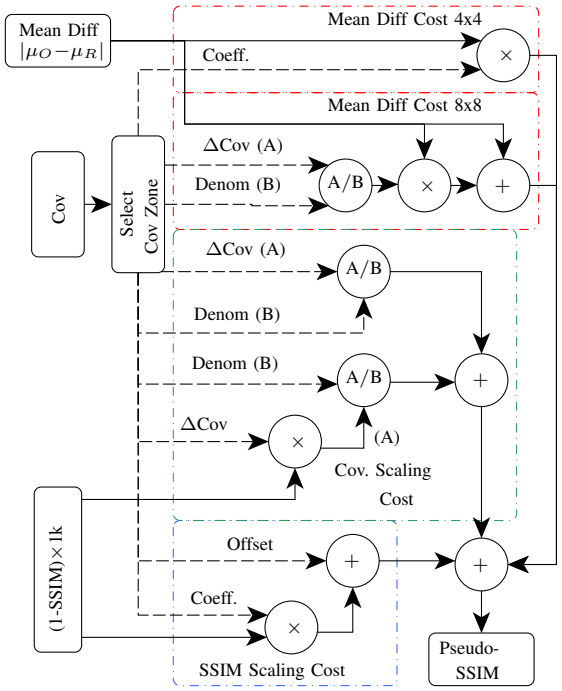

Fig. 7. Operational Block Diagram of PseudoSSIM

addresses these issues related to [8] by providing a general solution based upon modelling the UBR by block size [2]. This enables LHPSS to be integrated at the Sub-MB prediction and mode decision stages, thus awarding a distortion score based on the local perceptual significance. Furthermore, Pseudo-SSIM within LHPSS can be extended to dynamically adapt as described in equation (3)

From an operational point of view, Pseudo-SSIM can be seen to be competitive against STDMs. While an STDM would calculate the differences between a Original and Reconstructed block before determining the score, SSIM can be performed immediately before Pseudo-SSIM scales the SSIM value. However, where the SSIM or covariance values are out of range, it must then fall back to use SATD, an STDM. Therefore, for those values that fall out of scope of Pseudo-SSIM, the encoding process takes longer, thus requiring additional processing time.

V. Working of Pseudo-SSIM within LHPSS

The samples gathered to produce the scaled-SSIM-PDM model of Pseudo-SSIM were taken at the prediction level [2] based upon the data gathered from the first three frames of Foreman video sequence of QCIF resolution and reflect the large proportion low covariance regions shown in figure 4.

The internal processes involved to calculate Pseudo-SSIM are shown in figure 7. They comprise of three main parts, the Mean Difference Cost, the Covariance Scaling Cost and the SSIM Scaling Cost and together they sum up to output a Pseudo-SSIM score. There are six zones, which are set depending upon the covariance score, where ΔCov is the relative covariance that is subsequently processed. The weightings per covariance zone and SSIM profiles for Pseudo-SSIM are shown in tables II to XIV.

Within the Mean Difference Cost the pathways are specific to the block size. Specifically, the 8x8 Model, the mean difference can be high which will lead to addition processing of the mean difference towards the final value of the Mean Difference Cost. Otherwise, the Covariance Scaling Cost and SSIM Scaling Cost for both 4x4 and 8x8 block sizes are the same with only the values that differ. The values set for coefficients, denominator and offset within Pseudo-SSIM have been set to be either binary friendly or when applied implemented with as shifts, additions or subtractions. This has been possible by working with integers. The SSIM score is initially converted to $(1-\text{SSIM})\times 1000$ and covariance has had its respective covariance zones threshold subtracted and labelled as ΔCov. Thus, only when two unknowns at designed time are multiplied or SSIM is converted to $(1-\text{SSIM})\times 1000$ does a multiplication take place. Therefore, 4x4 block will undergo two multiplication operations and an 8x8 block will have three multiplication operations, The purposed of the covariance scaling cost is to distinguish two samples of same the SSIM value by their respective covariance within the distortion metric space of SATD. Hence, the upper part of ΔCov divided by a denominator factor states the position within the given zone. While the lower part of $\Delta\text{Cov}\times(1-\text{SSIM})\times 1000$ reflects how the zones are divided into SSIM bands and so this represents the rate of growth for the given band.

VI. Results

The results in table I show the implementation of the LHPSS at the Prediction and Mode Decision stages, operating as a distortion metric alternative to SATD where conditions are met. The performance results are from the encoder's console and statistics file and further analysis of the mode selection on the intra frame were extracted separately from the encoder.

The default configuration file in JM18.4 MPEG4/AVC [9] was set-up with the recommendations set by [10] and SSIM assessment. A separate modified JM18.4 code base with the LHPSS model implemented was set-up with the same configuration except for LHPSS operating at Motion Estimation (Half and Quarter Pixel) and at Mode Decision Distortion.

The video sequences selected are of HD resolution (1920x1080), 'CrowdRun' and 'sunflower', 50 and 25 frames/second respectively. The tests were run under 'IbBbBbBbP' and 'IPPP' prediction structure [10] across four Quantisation Parame (QP) values of 22, 27, 32 and 37 for QPISlice, with QPPSlice and QPBSlice increamented by 1, i.e. if QPISlice is 22, QPPSlice is 23 and QPBSlice is 24.

IbBbBbBbP					
CrowdRun	**QP22**	**QP27**	**QP32**	**QP37**	**Ave.**
Total Time	19.70%	19.70%	12.67%	21.07%	18.29%
Y-PSNR	-0.35%	-0.55%	-0.65%	-0.57%	-0.53%
Y-SSIM	-0.06%	-0.20%	-0.44%	-0.68%	-0.34%
Total Bits	1.95%	1.38%	0.53%	-0.54%	0.83%
Sunflower	**QP22**	**QP27**	**QP32**	**QP37**	**Ave.**
Total Time	21.16%	21.91%	23.50%	24.81%	22.85%
Y-PSNR	-0.19%	-0.30%	-0.34%	-0.43%	-0.31%
Y-SSIM	-0.03%	-0.07%	-0.16%	-0.39%	-0.16%
Total Bits	0.57%	-1.99%	-5.45%	-9.49%	-4.09%
IPPP					
CrowdRun	**QP22**	**QP27**	**QP32**	**QP37**	**Ave.**
Total Time	-5.51%	4.80%	10.39%	12.31%	5.50%
Y-PSNR	-31.17%	-32.74%	-35.15%	-38.56%	-34.40%
Y-SSIM	-16.96%	-25.68%	-35.48%	-46.88%	-31.25%
Total Bits	-82.97%	-83.33%	-82.34%	-84.37%	-83.25%
Sunflower	**QP22**	**QP27**	**QP32**	**QP37**	**Ave.**
Total Time	13.27%	19.29%	20.00%	23.90%	19.12%
Y-PSNR	-15.10%	-17.51%	-19.29%	-23.63%	-18.88%
Y-SSIM	-2.80%	-4.80%	-7.88%	-13.88%	-7.34%
Total Bits	-68.86%	-65.60%	-50.29%	-24.49%	-52.31%

TABLE I
SUMMARY OF LHPSS RELATIVE VIDEO PERFORMANCE SHOWN AS % DIFFERENCES FOR IBBBBBBBP AND IPPP PREDICTION STRUCTURE USING CROWDRUN AND SUNFLOWER 1080P

The run of tests were performed with Rate Distortion Optimisation (RDO) Quantisation (RDOQ) enabled, whereby each prediction mode is assessed by their Distortion Score as well as compressibility, reflecting the need to balance (R-D). The run of tests with RDOQ disabled have not been performed, since the results with RDOQ enabled would occupy a smaller range of SSIM, excluding the extreme cases and thus, increasing the likelihood of having those prediction modes that are closer to the origin of the R-D curve. The tests were performed using a system with an Intel Core i7 CPU 920 processor operating at 2.67GHz and 7GB of RAM.

VII. Encoder Performance

The novel LHPSS model has been implemented within the JM18.4 H.264/AVC Encoder as shown in figure 7.

The summary of results presented in table I, shows the performance of SATD and Pseudo-SSIM. The Encoder outputs information pertaining frame bit usage, timings and IQ. These are shown as relative video performance shown as % differences for IbBbBbBbP and IPPP prediction structure using CrowdRun and Sunflower 1080p.

The results for IbBbBbBbP prediction structure illustrate CrowdRun to have an overall bit usage approximately the same as SATD, within $\pm 2\%$, across the range of QP's tested. Similarly, the PSNR and SSIM values remain within 1% difference. Comparing to Sunflower, which is a highly textured video sequence, the bit usage progressively drops under LHPSS as

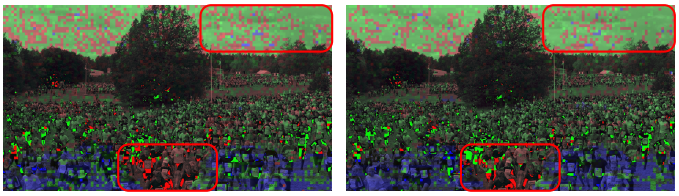

(a) SATD I4x4:57, I8x8:6408, I16x16:1695 (b) Pseudo-SSIM I4x4:67, I8x8:6161, I16x16:1932

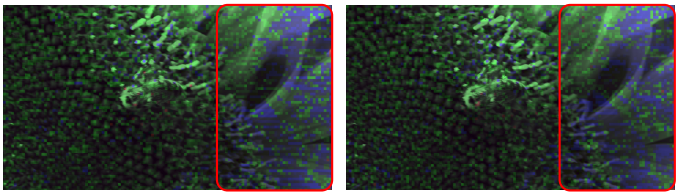

(c) SATD I4x4:2910, I8x8:4333, I16x16:917 (d) Pseudo-SSIM I4x4:2127, I8x8:4880, I16x16:1153

Fig. 8. CrowdRun (top pair) and Sunflower (bottom pair)Frame 1 (Intra) Luma with Highlighted Macroblocks type, Red for Intra4x4, Green for Intra 8x8 and Blue for Intra 16x16.

QP increases, while image quality (IQ) score dropping by less than $\frac{1}{2}\%$. The overall time for encoding the video sequence using the LHPSS model is $+18\%$ and $+23\%$ respectively for CrowdRun and Sunflower.

Under IPPP prediction structure, the overall bit usage dramatically drops by 83% and 52% respectively for CrowdRun and Sunflower; however, this happens at the expense of IQ. For CrowdRun, PSNR using LHPSS reduces by 31% at QP22 and 39% at QP37 when comparted to SATD. For Sunflower, the PSNR is 15% lower at QP22 and 24% lower at QP37 when LHPSS is used. In SSIM terms, the drop in IQ is on average almost a third in CrowdRun and a fifth in Sunflower.

The intra frame with mode selection superimposed on top is shown in figure 8. Here, a greater number of larger block sizes are chosen with LHPSS. In CrowdRun, the top 'sky' region, which is mainly homogeneous, shows a large number of 8x8 blocks (green) when compared to SATD. Also, in the middle front of the CrowdRun, the number of 4x4s used is less under LHPSS. In the Sunflower test video, the number of 16x16 is approximately 14% higher, which are largely concentrated on the petals on the right hand side. Again, this region is homogeneous, thus exploiting perceptual redundancy.

VIII. Conclusion and Future Work

The results presented in this paper have demonstrated that SSIM scaling by using its own component of 'covariance', both satisfies the Triangle Equality Rule ($\trianglelefteq$) and utilises a perceptual means of scaling.

The LHPSS model utilises non-logarithmic functions thus allowing for it to be implemented at the Sub Macroblock Prediction and Mode Decision stages of a block-based encoder. The model is based upon data which is gathered from the first three frames of the Foreman QCIF resolution video and subsequently tested on HD resolution against SATD to show the generalisation of the novel LHPSS model's applicability.

The results show the model is able to retain a level of IQ in IbBbBbBbP for similar or lower bit usage, though the time taken is high. For the IPPP prediction structure case, the bit usage is dramatically lowered at the expense of IQ, with time taken remaining high. The increase in time is related to LHPSS falling back on to SATD for those samples which SSIM or covariance values are out of scope of Pseudo-SSIM. While this novel approach shows a potential for bit-budget improvement, it can be refined with a more accurate model, which can address the IQ losses seen in IPPP. This can be addressed by extending the coverage of LHPSS to a wider range of SSIM and covariance from different video sources as discussed in [2]. Thus, produce a more accurate perceptual R-D model as mentioned in [3] as well as minimise the fall back to SATD, and so also address issues related to timing.

When the Intra frame image with the Mode Decision was shown, under LHPSS, homogeneous regions exhibited higher number of larger block sizes than SATD. This is encouraging, demonstrating that where the LHPSS model is successful in lowering the convex hull of the Rate-Distortion curve towards the origin. This work can be extended in the form of equation (3), so that Pseudo-SSIM adapts depending upon the perceptual nature of the block and the bit budget. Therefore, implementing a Local Perceptual Rate Control with a dynamically adapting perceptual distortion metric to complete the Perceptual Framework discussed in [2].

References

[1] H. Everett III, "Generalised Lagrange Multiplier Method for Solving Problems of Optimum Allocation of Resources," *Operations Research*, vol. 11, no. 3, pp. 399 – 417, 1963.

[2] Y. G. Joshi, P. Shah, J. Loo, and S. Rahman, "Review of Standard Traditional Distortion Metrics and a need for Perceptual Distortion Metric at a (Sub) Macroblock Level," in *IEEE International Symposium on Broadband Multimedia Systems and Broadcasting 2013*, June 2013.

[3] A. Ortega and K. Ramchandran, "Rate-distortion methods for image and video compression," *IEEE Signal Processing Magazine*, vol. 15, no. 6, pp. 23–50, 1998.

[4] G. Sullivan and T. Wiegand, "Rate-distortion optimization for video compression," *IEEE Signal Processing Magazine*, vol. 15, no. 6, pp. 74–90, 1998.

[5] T. Richter, "SSIM as Global Quality Metric: A Differential Geometry View," in *Proc. Third Int Quality of Multimedia Experience (QoMEX) Workshop*, 2011, pp. 189–194.

[6] C.-H. Chou and Y.-C. Li, "A Perceptually Tuned Subband Image Coder Based on the Measure of Just-Noticeable-Distortion Profile," *IEEE Transactions on Circuits and Systems for Video Technology*, vol. 5, no. 6, pp. 467–476, 1995.

[7] Z. Wang, A. C. Bovik, H. R. Sheikh, and E. P. Simoncelli, "Image Quality Assessment: From Error Visibility to Structural Similarity," *IEEE Transactions on Image Processing*, vol. 13, no. 4, pp. 600–612, 2004.

[8] Y.-H. Huang, T.-S. Ou, and H. Chen, "Perceptual-Based Coding Mode Decision," in *IEEE International Symposium on Circuits and Systems (ISCAS), Proceedings of 2010*, 302010-june2 2010, pp. 393 –396.

[9] K. Sühring. H.264/AVC Reference Software JM. [Online]. Available: http://iphome.hhi.de/suehring/tml/

[10] S. G. Tan T.K. and W. T., "(VCEG-AJ10r1) Recommended Simulation Common Conditions for Coding Efficiency Experiments Revision 4." ITU-T SC16/Q6, 36th VCEG Meeting, San Diego, USA, 8th - 10th Oct., 2008, 2008.

$\mathbf{x}_{min}$	$\mathbf{x}_{max}$	$\mathbf{SSIM}_{cost}$ **Offset**	**Coeff.**	$\mathbf{Cov}_{cost}$ **ΔCov×x**	**ΔCov**
2	10	8	1 1/8	1/64	1/32
10	20	12	3/4	1/128	1/8
20	50	14	5/8	1/256	3/16
50	100	32	1/4	1/256	1/4
100	200	32	1/4	1/1024	5/16
200	600	32	1/4	1/512	1/2
600	800	−300	3/4	1/256	−1/2
800	900	−1,688	2 1/2	1/64	−10

TABLE II

4X4: ZONE1$_{Cov}$ (0≤COV<150) WHERE X=(1−SSIM)×1K

$\mathbf{x}_{min}$	$\mathbf{x}_{max}$	$\mathbf{SSIM}_{cost}$ **Offset**	**Coeff.**	$\mathbf{Cov}_{cost}$ **ΔCov×x**	**ΔCov**
2	10	12	3 5/8	1/256	1/16
10	20	28	1 15/16	1/256	1/16
20	50	42	1 1/4	1/256	1/16
50	100	58	15/16	1/512	1/8
100	200	80	11/16	1/512	1/8
200	600	88	5/8	1/512	1/8
600	800	−142	1	1/512	1/8

TABLE III

4X4: ZONE2$_{Cov}$ (150≤COV<300) WHERE X=(1−SSIM)×1K

$\mathbf{x}_{min}$	$\mathbf{x}_{max}$	$\mathbf{SSIM}_{cost}$ **Offset**	**Coeff.**	$\mathbf{Cov}_{cost}$ **ΔCov×x**	**ΔCov**
0	2	32	3 5/8	1/256	1/64
2	10	32	3 5/8	1/256	1/32
10	20	40	2 1/2	1/256	1/32
20	50	56	1 3/4	3/1024	1/32
50	100	86	1 1/8	1/1024	1/8
100	200	102	15/16	1/2048	3/16
200	600	108	7/8	1/1024	3/32
600	800	−120	1 1/4	1/128	−4

TABLE IV

4X4: ZONE3$_{Cov}$ (300≤COV<600) WHERE X=(1−SSIM)×1K

$\mathbf{x}_{min}$	$\mathbf{x}_{max}$	$\mathbf{SSIM}_{cost}$ **Offset**	**Coeff.**	$\mathbf{Cov}_{cost}$ **ΔCov×x**	**ΔCov**
0	2	36	5 5/8	1/64	1/256
2	10	36	5 5/8	1/256	3/128
10	20	56	3 3/8	1/512	5/128
20	50	80	2 1/4	1/1024	1/16
50	100	124	1 3/8	1/1024	3/64
100	200	160	1 1/8	1/2048	3/32
200	600	160	1 1/16	1/2048	3/32

TABLE V

4X4: ZONE4$_{Cov}$ (600≤COV<1350) WHERE X=(1−SSIM)×1K

$\mathbf{x}_{min}$	$\mathbf{x}_{max}$	$\mathbf{SSIM}_{cost}$ **Offset**	**Coeff.**	$\mathbf{Cov}_{cost}$ **ΔCov×x**	**ΔCov**
0	2	48	8 1/2	3/256	−1/64
2	10	48	8 1/2	1/512	1/64
10	20	84	4 3/4	1/1024	7/256
20	50	120	3	1/1024	1/32
50	100	176	1 7/8	1/1024	3/128
100	200	214	1 1/2	(ΔCV/8)×x/2048	7/64
200	250	284	1 1/4	(ΔCV/8)×x/2048	3/32

TABLE VI

4X4: ZONE5$_{Cov}$ (1350≤COV<3014) WHERE X=(1−SSIM)×1K

$\mathbf{x}_{min}$	$\mathbf{x}_{max}$	$\mathbf{SSIM}_{cost}$ **Offset**	**Coeff.**	$\mathbf{Cov}_{cost}$ **ΔCov×x**	**ΔCov**
0	2	66	12	3/512	−1/256
2	10	66	12	1/512	1/512
10	20	128	6 3/4	(ΔCV/16)×x/512	1/64
20	50	186	4 1/4	(ΔCV/4)×x/512	1/128
50	100	256	3	(ΔCV/4)×x/512	1/256

TABLE VII

4X4: ZONE6$_{Cov}$ (3014≤COV<8000) WHERE X=(1−SSIM)×1K

$\mathbf{x}_{min}$	$\mathbf{x}_{max}$	$\mathbf{SSIM}_{cost}$ **Offset**	**Coeff.**	$\mathbf{Cov}_{cost}$ **ΔCov×x**	**ΔCov**
2	10	42	3 1/4	1/64	5/8
10	50	46	2 1/4	1/64	3/4
50	100	96	1 1/4	1/64	1
100	600	128	1	1/128	3/2
600	750	−350	1 3/4	1/64	−3 1/4
750	900	−2,375	4 1/2	1/128	2
900	975	−22,000	26	1/128	1

TABLE VIII

8X8: ZONE1$_{Cov}$ (0≤COV<150) WHERE X=(1−SSIM)×1K

$\mathbf{x}_{min}$	$\mathbf{x}_{max}$	$\mathbf{SSIM}_{cost}$ **Offset**	**Coeff.**	$\mathbf{Cov}_{cost}$ **ΔCov×x**	**ΔCov**
2	10	150	5 1/2	1/16	1/4
10	50	150	5 1/2	1/64	1/8
50	100	192	4 1/2	1/512	1
100	600	256	2 1/2	1/256	1
600	900	−1,024	4 1/2	1/128	−1

TABLE IX

8X8: ZONE2$_{Cov}$ (150≤COV<300) WHERE X=(1−SSIM)×1K

$\mathbf{x}_{min}$	$\mathbf{x}_{max}$	$\mathbf{SSIM}_{cost}$ **Offset**	**Coeff.**	$\mathbf{Cov}_{cost}$ **ΔCov×x**	**ΔCov**
2	10	100	9	1/32	3/16
10	20	100	9	1/32	1/8
20	50	100	9	0	5/8
50	100	312	4	1/128	3/8
100	500	448	3	1/256	1/2
500	600	448	3	1/128	−3/2
600	750	−600	5	1/256	1/2

TABLE X

8X8: ZONE3$_{Cov}$ (300≤COV<600) WHERE X=(1−SSIM)×1K

$\mathbf{x}_{min}$	$\mathbf{x}_{max}$	$\mathbf{SSIM}_{cost}$ **Offset**	**Coeff.**	$\mathbf{Cov}_{cost}$ **ΔCov×x**	**ΔCov**
0	10	168	16 1/2	1/64	1/16
10	20	224	13 1/2	1/128	1/8
20	50	352	7	1/128	1/8
50	100	448	6	1/1024	3/8
100	550	552	4 3/4	1/512	1/4

TABLE XI

8X8: ZONE4$_{Cov}$ (600≤COV<1350) WHERE X=(1−SSIM)×1K

$\mathbf{x}_{min}$	$\mathbf{x}_{max}$	$\mathbf{SSIM}_{cost}$ **Offset**	**Coeff.**	$\mathbf{Cov}_{cost}$ **ΔCov×x**	**ΔCov**
0	10	245	30	1/128	1/32
10	15	368	17	1/128	1/64
15	20	368	17	1/256	1/16
20	50	464	12	1/256	1/16
50	100	464	12	−1/1024	5/16
100	275	848	6	1/256	0

TABLE XII

8X8: ZONE5$_{Cov}$ (1350≤COV<3014) WHERE X=(1−SSIM)×1K

$\mathbf{x}_{min}$	$\mathbf{x}_{max}$	$\mathbf{SSIM}_{cost}$ **Offset**	**Coeff.**	$\mathbf{Cov}_{cost}$ **ΔCov×x**	**ΔCov**
0	15	272	44	1/1024	1/128
15	50	512	20	1/512	1/64
50	200	952	10	1/1024	1/16

TABLE XIII

8X8: ZONE6$_{Cov}$ (3014≤COV<8000) WHERE X=(1−SSIM)×1K

Zone	**ΔCov Thresh**	**4x4: Coeff.**	**8x8:** $(Ax+B)\times\mu_\Delta+\mu_\Delta$
1	0	8	A: 1/16, B: 0
2	150	8	A: 1/16, B: 0
3	300	8	A: 7/128, B: -4
4	600	8	A: 3/512, B:16
5	1350	8	A: 5/512, B:2
6	3014	4	A: 5/512, B:-43

TABLE XIV

MEAN ABSOLUTE DIFFERENCE COST WHERE $\mu_\Delta = |\mu_{O-R}|$